Crystal Engineering

International Edition: DOI: 10.1002/anie.201901739
German Edition: DOI: 10.1002/ange.201901739

Chemistry Design Towards a Stable Sulfide-Based Superionic Conductor $Li_4Cu_8Ge_3S_{12}$

Yingqi Wang, Xujie Lü, Chong Zheng, Xiang Liu, Zonghai Chen, Wenge Yang,* Jianhua Lin, and Fuqiang Huang**

Abstract: *Sulfide-based superionic conductors with high ionic conductivity have been explored as candidates for solid-state Li batteries. However, moisture hypersensitivity has made their manufacture complicated and costly and also impeded applications in batteries. Now, a sulfide-based superionic conductor $Li_4Cu_8Ge_3S_{12}$ with superior stability was developed based on the hard/soft acid–base theory. The compound is stable in both moist air and aqueous LiOH aqueous solution. The electrochemical stability window was up to 1.5 V. An ionic conductivity of 0.9×10^{-4} S cm with low activation energy of 0.33 eV was achieved without any optimization. The material features a rigid Cu-Ge-S open framework that increases its stability. Meanwhile, the weak bonding between Li^+ and the framework promotes ionic conductivity. This work provides a structural configuration in which weak Li bonding in the rigid framework promotes an environment for highly conductive and stable solid-state electrolytes.*

Lithium-ion batteries (LIBs) are used to power billions of portable electronic devices and electric vehicles, and are therefore of great importance in modern society. Nevertheless, the organic electrolytes in current commercialized LIBs bring safety issues such as leakage, poor chemical stability, and high flammability. Replacing liquid electrolytes with solid-state inorganic electrolytes has been considered the ultimate solution to address the safety issues.[1] Moreover, using solid-state electrolytes for all-solid-state LIBs enable higher energy density, power density, and better-fitting flexible devices.[2] In the past, studies of solid electrolytes focused largely on lithium conducting oxides, such as LISICON,[3] LiPON,[4] garnet,[5] perovskite,[6] and anti-perovskite systems.[7] High fast-ion conduction were found in some sodium and lithium salts with a large anion cluster, such as $LiCB_{11}H_{12}$ and $Na_2B_{12}H_{12}$.[8] However, a transition temperature, usually higher than room temperature, is needed to activate these materials. Recently, significant progress has been made with the discovery of a serious of sulfide-based ionic conductors, including thio-LISICON, $Li_7P_3S_{11}$,[9] and $Li_{10}GeP_2S_{12}$.[10] These compounds exhibit high ionic conductivities, some of which even outperform conventional liquid electrolytes.[10]

Despite the tremendous success in improving lithium ionic conductivity, sulfide-based solid electrolytes still face the considerable challenge of hypersensitivity to air and moisture.[11] When exposed to an ambient environment even for a short time, they will hydrolyze rapidly, leading to the release of noxious H_2S gas, and a tremendous decrease in their lithium ionic conductivity. Such instability issues increase the processing cost and make them impractical for some new battery configurations, such as an aqueous battery and redox flow batteries.[12] To date, successful examples of sulfide-based electrolytes that tolerate exposure to water are rare.[13,12a] Another critical factor for designing a superionic conductor is the coordination environment of lithium, which directly affects the ion migration and activation. It has been proposed that the unfavorable coordination of the mobile ion can potentially lead to high mobility, and low activation energy,[10,14] but the thermodynamic instability causes difficulties in material synthesis. Mobile cations in most reported sulfide-based superionic conductors adopt tetrahedral or octahedral sites, which usually has strong bonding interaction. Therefore, it is essential to explore other coordination structures where Li-ions have weak bonding interaction and thus, can bring about high ionic conductivity.

Based on the hard/soft acid–base (HSAB) theory,[15] relatively soft acids such as Ge^{IV} and Cu^{I} prefer soft bases such as S^{2-}, forming strong covalent bonds and a rigid framework. By further introducing open channels for the migration of ions, such a structure can be a promising candidate for superionic conductor. Herein, we report the

[*] Dr. Y. Wang, X. Lü, W. Yang
Center for High Pressure Science & Technology Advanced Research
Shanghai 206203 (P. R. China)
E-mail: xujie.lu@hpstar.ac.cn
yangwg@hpstar.ac.cn
Prof. J. Lin, Prof. F. Huang
State Key Laboratory of Rare Earth Materials Chemistry and Applications, College of Chemistry and Molecular Engineering
Peking University, Beijing 100871 (P. R. China)
E-mail: huangfq@pku.edu.cn
Prof. F. Huang
CAS Key Laboratory of Materials for Energy Conversion
Shanghai Institute of Ceramics, Chinese Academy of Sciences
Shanghai 200050 (P. R. China)
Prof. C. Zheng
Department of Chemistry and Biochemistry
Northern Illinois University, DeKalb, IL 60115 (USA)
X. Liu, Dr. Z. Chen
Chemical Sciences and Engineering Division
Argonne National Laboratory, Lemont, IL 60439 (USA)
Supporting information and the ORCID identification number(s) for the author(s) of this article can be found under: https://doi.org/10.1002/anie.201901739.

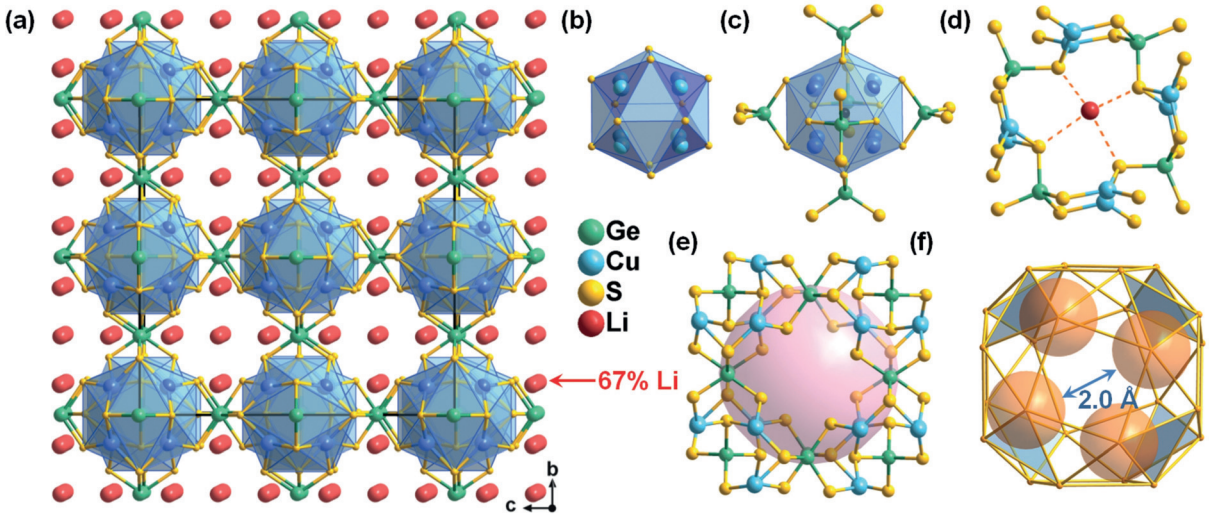

Figure 1. Crystal structure of $Li_4Cu_8Ge_3S_{12}$. a) The structure viewed along the [100] direction. b) The model of the $[Cu_8S_{12}]^{16-}$ icosahedral cluster and c) its connectivity with the $[GeS_4]^{4-}$ tetrahedra. d) Square pyramidal coordination of the Li^+ ion at the window of the anion framework cavity with 66.7% occupancy. e) $[Cu_8Ge_6S_{24}]^{16-}$ clusters form a 6.8 Å diameter cavity, and f) 3D channels of 2.0 Å in window size considering the radius of S^{2-}.

design of a new compound $Li_4Cu_8Ge_3S_{12}$ (LCGS) featuring a stable and open Cu-Ge-S framework, in which Li^+ ions are weakly bonded. LCGS shows high stability with an ionic conductivity of 0.9×10^{-4} S cm and activation energy of 0.33 eV without any optimization. We hereby propose an effective way to design the coordination environment of mobile ions, and thus open up a broader scope for the crystal design and structure search towards high-performance solid electrolytes.

LCGS was synthesized via urothermal conditions at 200 °C (Supporting Information). Both powder and single-crystal X-ray diffraction (XRD) were used to characterize the crystal structure, as shown in the Supporting Information, Figure S2 and Table S2.[25] LCGS adopts the space group of $Fm\bar{3}c$ (226) where Cu, Ge, and S construct an anionic skeleton while the lithium ions occupy the void space of the open framework (Figure 1 a). The overall three-dimensional (3D) structure can be viewed as primitive cubic packing of icosahedral $[Cu_8S_{12}]^{16-}$ clusters (Figure 1 b) linked with $[GeS_4]^{4-}$ tetrahedra via edge sharing (Figure 1 c). The resulting 3D open framework exhibits a cavity of 6.8 Å in diameter, and 3D channels of 2.0 Å in tunnel size (Figures 1 e,f), which is larger than the 1.5 Å ionic diameter of Li^+.[16] Four Li ions are statistically distributed over six equivalent cavity positions with an occupancy of 2/3. Distinguished from most sulfide and oxide electrolytes in which lithium ions are tetrahedrally or octahedrally coordinated with the anions, the Li ions in the LCGS structure reside at the planar square tunnel of the cavity, forming square pyramid coordination with four sulfides. The Li–S distances are 3.33(1) Å, which is longer than the typical bond lengths of 2.2–2.9 Å (Supporting Information, Table S3). Such square pyramid coordination of Li^+ is thermodynamically less stable than tetragonal or octahedral coordination. Thus, the weakly bonded Li ions can migrate more easily in the 3D connected sulfide open framework. In contrast with the unstable coordination of counter ion Li^+, the strong covalent bonding of Cu–S and Ge–S in the rigid anionic framework keeps the structural integrity of LCGS during Li ion transport. Meanwhile, the relatively high ratio of vacancy (33.3%) enhances the lithium ionic hoping probability.[7a] The difference electron density map of the structure (F_{diff}) at the $z=0.25$ xy plane was obtained by Fourier transforming the single-crystal data (Figure 2). Large and diffused electron density was located around the Li site (48*f*, 0.25 0.41 0.25), suggesting a 3D conduction pathway. The diffused electron density along the pathway also indicates high Li-ion mobility with a low energy barrier, which is similar to that found in some sodium chalcogenide superionic conductor crystals.[17]

In some copper chalcogenides, Cu can adopt a mixed valence of +1 and +2, resulting in different occupancy of the alkali counterions. Since XRD cannot accurately determine the occupancy of Li owing to its diffuse nature, X-ray

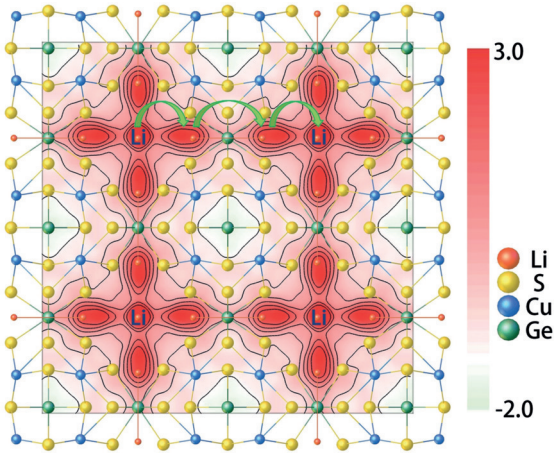

Figure 2. Difference Fourier map of the structure (F_{diff}) at the $z=0.25$ xy plane obtained from single-crystal data.

photoelectron spectroscopy (XPS) and inductively coupled plasma–atomic emission spectroscopy (ICP-AES) were used to verify the state of Cu and concentration of Li^+. As shown in the Supporting Information, Figure S5, the single symmetric peak of Cu $2P_{3/2}$ with a binding energy of 932.0 and 951.8 eV confirms that only Cu^+ exists in LCGS. ICP-AES gives a ratio Li/Cu/Ge of 3.9:8.05:2.93 (Supporting Information, Table S3), matching the theoretical formula $Li_4Cu_8Ge_3S_{12}$. Thus, the occupancy of Li^+ at site 48*f* is 67%, which is important for the migration of lithium ions.

Impedance spectroscopy was used to study the ionic conductivity of LCGS, and the result is shown in Figure 3a.

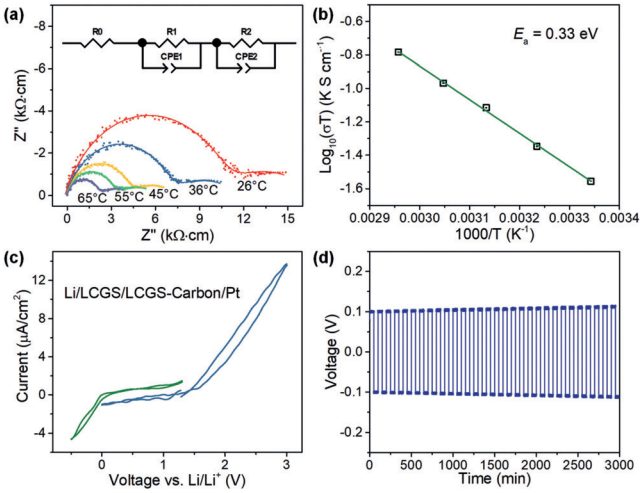

Figure 3. Electrochemical properties of LCGS. a) Nyquist plots of the AC impedance data from low to high temperatures. The inset shows the equivalent circuit. b) Arrhenius conductivity plot gives an activation energy $E_a = 0.33$ eV. c) Cyclic voltammetry measurement of Li/LCGS/LCGS-Carbon/Pt cell at a scan rate of 0.1 mV s^{-1} in the voltage range of 0–3 V and −0.5–1.25 V. d) Direct current (DC) polarization curve of the Li/$Li_4Cu_8Ge_3S_{12}$/Li symmetric cell cycled at a current density of 0.1 mA cm^{-2}, illustrating good compatibility with Li metal.

The spectra feature a semicircle and a spike in the high-frequency and low-frequency regions, corresponding to the contribution from the bulk/grain boundary and the electrode, respectively.[18] The ionic conductivity of LCGS calculated from the sum of the grain boundary and bulk resistance is 0.9×10^{-4} S cm at room temperature. The activation energy (E_a) is obtained from the slope of the Arrhenius plot (Figure 3b) based on the equation $\sigma T = A \exp(-E_a/k_B T)$, where k_B is the Boltzmann constant, T is the measured temperature, and σ is the ionic conductivity. The E_a of LCGS is derived as 0.33 eV, which is comparable to that of the state-of-the-art sulfide-based superionic conductors.[11] The relatively high ionic conductivity and low activation energy are due to the vacancies and weak bonding of Li^+ to the 3D channels of this well-designed structure.

The electrical conductivity ($\sigma_{dc\text{-}electron}$) of LCGS was determined by DC polarization measurement (Supporting Information, Figure S6), which gave a very low value of 3.6×10^{-7} S cm. The low electrical conductivity prevents self-discharging in solid-state Li batteries. The Li-ion transfer number (t_{ion}) was calculated to be 0.996 according to the equation $t_{ion} = (\sigma_{dc\text{-}Li} - \sigma_{dc\text{-}electron})/\sigma_{dc\text{-}Li}$,[19] where $\sigma_{dc\text{-}Li}$ stands for the DC Li ionic conductivity, and can be estimated to be 0.4×10^{-4} S cm from the DC polarization curve of the Li/$Li_4Cu_8Ge_3S_{12}$/Li symmetric cell (Figure 3d). The close-to-unity t_{ion} suggests that LCGS is a pure lithium ion conductor.[18]

The electrochemical stability of LCGS was evaluated by cyclic voltammetry (CV) using a Pt/Carbon-LCGS/LCGS/Li asymmetric cell at a scan rate of 0.1 mV s^{-1} (Figure 3c).[20] The conductive carbon was mixed into the electrolyte LCGS to increase contact and active area, thus improve the kinetics of the decomposition reaction owing to the facile electron transport. No additional current peaks were detected in the scanned voltage range, which suggests that LCGS is stable against Li metal anode. Since the compatibility with Li anode is important for high-energy SSE cells, LCGS can avoid building up thick passivation layer against Li metal anode, which usually increases the interphase impedance. On the other hand, the LCGS electrolyte was gradually oxidized from around 1.5 V, indicated by the increasing of current density (Figure 3c, blue line). The thermodynamic stability against oxidation under high voltage still remains a key drawback of sulfide electrolytes today.[21] Strategies such as the interface engineering could be applied to extend the electrochemical stability of the electrolyte.[2,20,22]

To confirm the compatibility of LCGS with Li metal further, Li/LCGS/Li symmetric cells were fabricated and cycled at a current density of 0.1 mA cm^{-2} with a periodically changing polarity. Figure 3d shows the voltage profile of the cell cycled continuously for 50 h (100 min per cycle), where the voltage remained almost unchanged during cycling. This suggests that LCGS has outstanding stability in contact with Li metal during cycling. Since there are 33% of vacancies on the Li sites in LCGS, an excess of Li can intercalate into these vacancies without affecting the structural integrity when working with the Li metal electrode.

The stability of the solid electrolyte is highly desirable. It not only reduces the production cost but also allows for applications in various battery designs such as aqueous lithium batteries. Prevailing sulfide-based ionic conductors such as the Li-Ge-P-S system are prone to decomposition in moisture owing to the high affinity of hard acids (for example, phosphor) towards oxygen in water according to the HSAB theory.[13,23] Unlike the well-known Li-Ge-P-S system, we chose a soft acid, Cu^I, in our design to replace the hard acid P^V to construct a more stable sulfide skeleton. The existence of water in LCGS synthesis indicates higher stability of our material against moisture. We examined the stability of LCGS in moist air and aqueous solution conditions experimentally.

Water molecules could be absorbed into the pores of the framework during synthesis or exposure to air. However, the stable framework and weak coordination between water and Li^+ make it possible to remove the water. Thermal gravimetric analysis (TGA) shows that the absorbed water can be removed by heating in an Ar flow (Supporting Information, Figure S3). Powder XRD measured immediately after heating confirmed a retained crystal structure after water desorption (Supporting Information, Figure S4).

The structural stability of LCGS was examined under two conditions: 1) air exposure in a desiccator with about 15% humidity, and 2) exposure to a 2 M LiOH aqueous solution. After 24 hours of exposure, all samples were washed with absolute ethanol and then dried in vacuum at 60 °C for 4 hours to remove the residual moisture. Figure 4a shows the XRD patterns of pristine LCGS, the samples after exposure to air, and the LiOH solution. As expected, all the peaks remain the same as the pristine sample after treatment, indicating that the as-designed crystal structure is highly stable in conditions where most of the sulfide-based electrolytes cannot survive.

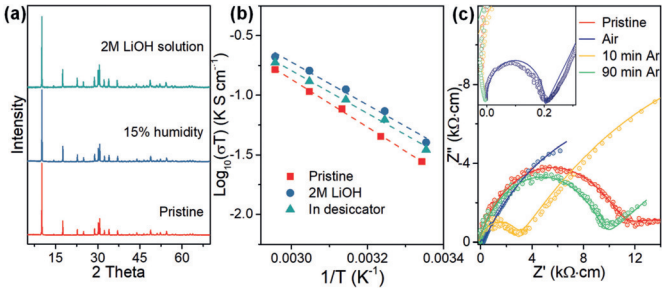

Figure 4. Chemical stability evaluation of LCGS. a) XRD patterns of LCGS before and after exposure in 15% moist air and a 2 M LiOH aqueous solution. b) Comparative Arrhenius plots show a minor change in conductivity and activation energy before and after exposure. c) Reversible variations of ionic conductivity for LCGS when exposed to moist air. The inset shows the magnified impedance plot.

The ionic conductivity of the pristine and the treated samples was measured by AC impedance spectroscopy. The room-temperature ionic conductivities of LCGS before treatment and after exposure to moist air or LiOH solution were 0.9×10^{-4} S cm, 1.2×10^{-4} S cm, and 1.3×10^{-4} S cm, respectively (Figure 4b). The activation energies of the pristine sample or samples treated in moist air and LiOH solution were derived as 0.33, 0.31, and 0.32 eV, respectively. Only minor changes in the conductivity and activation energy were observed, which means that the exposure in low moisture air and LiOH solution does not affect the intrinsic structure and electrochemical properties of LCGS.

To further investigate the reversible change of LCGS upon exposure to air, in situ impedance spectroscopy were compared for an LCGS pellet 1) in Ar flow, 2) in air exposure, 3) in Ar flow for 10 minutes after air exposure, and 4) in Ar flow for 90 minutes after air exposure. As shown in Figure 4c, the ionic conductivity increased significantly after exposure to moist air. The ionic conductivity increase is closely related to the air humidity (Supporting Information, Figure S7), which is probably due to the proton conductivity when water molecules were absorbed.[24] The ionic conductivity gradually decreased after the sample was re-blown in a continuous Ar flow (Figure 4c, yellow line: in Ar for 10 min after air exposure). The original ionic conductivity almost retained after 90 minutes owing to the loss of the adsorbed water. The minor change compared to the pristine sample may come from the small amount of remaining water, which can be removed by heating in an Ar flow (Supporting Information, Figure S3). This is superior to most of the sulfide-based solid electrolytes, which will decompose and their structure and electrochemical stability will be destroyed in humid air.[7c,11] All these results indicate the rigidity of LCGS framework, which gives rise to outstanding stability for potential energy-storage applications.

The coordination environment determines the stability and electrochemical properties of LCGS. According to the HSAB theory, relatively soft acids like Cu^{I} and Ge^{IV} form strong covalent bonds with soft base S^{2-}. The strong and rigid covalent framework, therefore, has low affinity to oxygen from air and water, leading to the superior stability of the structural skeleton in moist air or aqueous solutions. The openness of the framework allows for reversible water adsorption and desorption without changing the structure. The stability against water and ease of removing adsorbed moisture makes LCGS a robust and encouraging choice of solid-state electrolyte.

In conclusion, a sulfide-based superionic conductor, $Li_4Cu_8Ge_3S_{12}$, with superior stability and Li ionic conductivity was designed based on HSAB theory. A rigid Cu-Ge-S anionic open framework provides a rigid and stable scaffold. Li^+ ions sit in the channels with weak bonding and 33% vacancies. No significant redox reaction were observed by CV measurement in electrochemical window of 0–1.5 V. Moreover, LCGS exhibits exceptional chemical stability in air and LiOH aqueous solution with reversible water absorption and desorption. An ionic conductivity of 0.9×10^{-4} S cm at room temperature and an activation energy of 0.33 eV have been achieved. This work demonstrates a coordination chemistry design towards highly stable sulfide-based superionic conductors with high Li^+ conductivity. We believe that it is an encouraging step toward screening and designing more diversified crystal structure for solid-state lithium electrolytes.

Acknowledgements

This work was financially supported by National Natural Science Foundation of China (Grants U1530402, Y93GJ11101), China Scholarship Council and US Department of Energy, Vehicle Technologies Office (Contract No. DE-AC02-06CH11357).

Conflict of interest

The authors declare no conflict of interest.

Keywords: chalcogenide open frameworks · crystal engineering · enhanced stability · solid electrolytes · superionic conductors

How to cite: *Angew. Chem. Int. Ed.* **2019**, *58*, 7673–7677
Angew. Chem. **2019**, *131*, 7755–7759

[1] a) J. B. Goodenough, K.-S. Park, *J. Am. Chem. Soc.* **2013**, *135*, 1167; b) J. C. Bachman, et al., *Chem. Rev.* **2016**, *116*, 140; c) X. Lü, et al., *Adv. Sci.* **2016**, *3*, 1500359.

[2] J. Janek, W. G. Zeier, *Energy* **2016**, *500*, 300.
[3] P. Bruce, A. West, *J. Solid State Chem.* **1982**, *44*, 354.
[4] X. Yu, J. Bates, G. Jellison, F. Hart, *J. Electrochem. Soc.* **1997**, *144*, 524.
[5] Y. Li, et al., *Angew. Chem. Int. Ed.* **2017**, *56*, 753; *Angew. Chem.* **2017**, *129*, 771.
[6] J. A. Alonso, J. Sanz, J. Santamaría, C. León, A. Várez, M. T. Fernández-Díaz, *Angew. Chem. Int. Ed.* **2000**, *39*, 619; *Angew. Chem.* **2000**, *112*, 633.
[7] a) Y. Zhao, L. L. Daemen, *J. Am. Chem. Soc.* **2012**, *134*, 15042; b) X. Lü, G. Wu, J. W. Howard, A. Chen, Y. Zhao, L. L. Daemen, Q. Jia, *Chem. Commun.* **2014**, *50*, 11520; c) Y. Li, et al., *Angew. Chem. Int. Ed.* **2016**, *55*, 9965; *Angew. Chem.* **2016**, *128*, 10119; d) H. Fang, P. Jena, *Proc. Natl. Acad. Sci. USA* **2017**, *114*, 11046; e) J. A. Dawson, T. S. Attari, H. Chen, S. P. Emge, K. E. Johnston, M. S. Islam, *Energy Environ. Sci.* **2018**, *11*, 2993.
[8] a) W. S. Tang, A. Unemoto, W. Zhou, V. Stavila, M. Matsuo, H. Wu, S.-i. Orimo, T. J. Udovic, *Energy Environ. Sci.* **2015**, *8*, 3637; b) T. J. Udovic, et al., *Adv. Mater.* **2014**, *26*, 7622.
[9] H. Yamane, M. Shibata, Y. Shimane, T. Junke, Y. Seino, S. Adams, K. Minami, A. Hayashi, M. Tatsumisago, *Solid State Ionics* **2007**, *178*, 1163.
[10] Y. Wang, W. D. Richards, S. P. Ong, L. J. Miara, J. C. Kim, Y. Mo, G. Ceder, *Nat. Mater.* **2015**, *14*, 1026.
[11] A. Manthiram, X. Yu, S. Wang, *Nat. Rev. Mater.* **2017**, *2*, 16103.
[12] a) C. Ma, E. Rangasamy, C. Liang, J. Sakamoto, K. L. More, M. Chi, *Angew. Chem. Int. Ed.* **2015**, *54*, 129; *Angew. Chem.* **2015**, *127*, 131; b) Y. Zhao, Y. Ding, Y. Li, L. Peng, H. R. Byon, J. B. Goodenough, G. Yu, *Chem. Soc. Rev.* **2015**, *44*, 7968.
[13] G. Sahu, Z. Lin, J. Li, Z. Liu, N. Dudney, C. Liang, *Energy Environ. Sci.* **2014**, *7*, 1053.
[14] a) P. Canepa, et al., *Nat. Commun.* **2017**, *8*, 1759; b) Z. Rong, R. Malik, P. Canepa, G. S. Gautam, M. Liu, A. Jain, K. Persson, G. Ceder, *Chem. Mater.* **2015**, *27*, 6016.
[15] R. G. Pearson, *J. Chem. Educ.* **1968**, *45*, 581.
[16] R. D. Shannon, *Acta Crystallogr. Sect. A* **1976**, *32*, 751.
[17] a) L. Zhang, K. Yang, J. Mi, L. Lu, L. Zhao, L. Wang, Y. Li, H. Zeng, *Adv. Energy Mater.* **2015**, *5*, 1501294; b) N. Tanibata, K. Noi, A. Hayashi, N. Kitamura, Y. Idemoto, M. Tatsumisago, *ChemElectroChem* **2014**, *1*, 1130.
[18] P. Zhou, J. Wang, F. Cheng, F. Li, J. Chen, *Chem. Commun.* **2016**, *52*, 6091.
[19] E. Rangasamy, G. Sahu, J. K. Keum, A. J. Rondinone, N. J. Dudney, C. Liang, *J. Mater. Chem. A* **2014**, *2*, 4111.
[20] F. Han, Y. Zhu, X. He, Y. Mo, C. Wang, *Adv. Energy Mater.* **2016**, *6*, 1501590.
[21] a) T. Hakari, et al., *Chem. Mater.* **2017**, *29*, 4768; b) Y. Zhu, X. He, Y. Mo, *ACS Appl. Mater. Interfaces* **2015**, *7*, 23685.
[22] S. H. Jung, K. Oh, Y. J. Nam, D. Y. Oh, P. Brüner, K. Kang, Y. S. Jung, *Chem. Mater.* **2018**, *30*, 8190.
[23] H. Wang, Y. Chen, Z. D. Hood, G. Sahu, A. S. Pandian, J. K. Keum, K. An, C. Liang, *Angew. Chem. Int. Ed.* **2016**, *55*, 8551; *Angew. Chem.* **2016**, *128*, 8693.
[24] a) H. Xu, S. Tao, D. Jiang, *Nat. Mater.* **2016**, *15*, 722; b) X. Meng, H.-N. Wang, S.-Y. Song, H.-J. Zhang, *Chem. Soc. Rev.* **2017**, *46*, 464; c) G. K. Shimizu, J. M. Taylor, S. Kim, *Science* **2013**, *341*, 354; d) M. Yoon, K. Suh, S. Natarajan, K. Kim, *Angew. Chem. Int. Ed.* **2013**, *52*, 2688; *Angew. Chem.* **2013**, *125*, 2752.
[25] Further details on the crystal structure investigation may be obtained from the Fachinformationszentrum Karlsruhe, 76344 Eggenstein-Leopoldshafen, Germany (fax: (+49)7247-808-666; e-mail: crysdata@fiz-karlsruhe.de), on quoting the depository number CSD-1895407.

Manuscript received: February 8, 2019
Revised manuscript received: March 28, 2019
Accepted manuscript online: April 2, 2019
Version of record online: April 29, 2019

